Alexandria Engineering Journal (2021) 60, 1851–1860

HOSTED BY

ELSEVIER

Alexandria University

Alexandria Engineering Journal

www.elsevier.com/locate/aej
www.sciencedirect.com

Thermophoresis particle deposition analysis for nonlinear thermally developed flow of Magneto-Walter's B nanofluid with buoyancy forces

Yu-Ming Chu [a,b], Nargis Khan [c], M. Ijaz Khan [d,*], Kamel Al-Khaled [e], Nasreen Abbas [c], Sami Ullah Khan [f], Muhammad Sadiq Hashmi [g], Sumaira Qayyum [h], S. Kadry [i]

[a] *Department of Mathematics, Huzhou University, Huzhou 313000, PR China*
[b] *Hunan Provincial Key Laboratory of Mathematical Modeling and Analysis in Engineering, Changsha University of Science & Technology, Changsha 410114, PR China*
[c] *Department of Mathematics, The Islamia University of Bahawalpur, Pakistan*
[d] *Department of Mathematics and Statistics, Riphah International University I-14, Islamabad 44000, Pakistan*
[e] *Department of Mathematics & Statistics, Jordan University of Science and Technology, P.O. Box 3030, Irbid 22110, Jordan*
[f] *Department of Mathematics, COMSATS University Islamabad, Sahiwal 57000, Pakistan*
[g] *Department of Mathematics, The Govt. Sadiq College Women University, Bahawalpur, Pakistan*
[h] *Department of Mathematics, Quaid-I-Azam University, Islamabad 44000, Pakistan*
[i] *Department of Mathematics and Computer Science, Beirut Arab University, Beirut, Lebanon*

Received 23 September 2020; revised 24 October 2020; accepted 14 November 2020
Available online 5 December 2020

KEYWORDS

Walter's nanofluid;
Brownian motion and thermophoresis diffusion;
Chemical reaction;
Nonlinear thermal radiation;
Convective boundary conditions;
Joule heating

Abstract In this study, we have discussed thermophoresis particle deposition effects under the action of both pressure and buoyant forces flow of magneto-Walter's B nanofluid induced by a stretched surface. The Buongiorno nanofluid model is employed to analyze the dynamic impact of thermophoretic dispersion and Brownian motion. The effects of chemical reaction, Joule heating and non-linear radiation relations are also incorporated. The analysis has been performed in view of solutal and heat convective boundary constraints. The analytical technique namely homotopy analysis scheme followed to solve the resulting non-linear governing equations. The behavior of velocity, temperature and concentration profiles are observed graphically. The physical consequences for all physical parameters are justified. It is noted that heat thermal Biot number, thermophoretic constant and viscoelastic parameter increases the nanofluid temperature and concentration. A decaying concentration profile is noted for Schmidt number.

* Corresponding author.
E-mail address: mikhan@math.qau.edu.pk (M. Ijaz Khan).

Peer review under responsibility of Faculty of Engineering, Alexandria University.

https://doi.org/10.1016/j.aej.2020.11.033
1110-0168

Nomenclature

(u, v)	velocity components along x and y axes (ms^{-1})	T	temperature (K)
D_T	thermophoretic diffusion coefficient (kg/msK)	T_∞	ambient temperature (K)
T_w	wall temperature (K)	k	conductivity (m^2 s^{-1})
h_1	heat transfer coefficient	D_B	Brownian diffusion coefficient (kg/ms)
C	concentration (W/m^2 K)	M	Hartman number
β	material parameter	η	chemical heat generation parameter
λ	thermal buoyancy parameter	J	thermophoretic parameter
Le	Lewis number	N_b	Brownian motion parameter
Pr	is the Prandtl	N_t	thermophoresis parameter
R	thermal radiation parameter	γ_1	thermal Biot number
Ec	Eckert number	Sc	Schmidt number
δ	heat generation parameter and		
g	acceleration due to gravity (ms^{-2})		

1. Introduction

The novel and distinct dynamic of non-Newtonian fluids attained attention of scientists because of their noteworthy importance in manufacturing and processing industries, medical sciences, technological applications and food industries. The non-Newtonian fluid include valuable applications in bio-engineering, food processing, blood, chemical processes, oil refineries, biological liquids, polymer liquids, aerodynamic extrusion, paints etc. Owing to complicated and multidisciplinary nature of non-Newtonian materials, researchers have introduced different relations to examine the clear insight feature of such materials. Out of diverse nonlinear models imposed in already reported literature, Walter's-B liquid is one which belongs to the differential type fluids and intended the investigators attention due to its complex features. The magnetized flow of Walter's-B fluid shows dynamic applications in lubrications, plasma, refrigeration, MHD pumps etc. Beard and Walter [1] conducted basic work on Walter's B non-Newtonian material which was further extended by many researchers [2-4].

In industrial processes, the cooling of microelectronic devices has a significant part. The base fluids similar to oil, ethylene glycol and water with lower thermal conductivity has numerous restrictions. By inserting nano-size particles into base fluid since liquids can be established. The insertion of these elements varies thermo physical proficiency of fluids. We cannot find this types of liquids certainly but can be finding in laboratories. Thermal implementation of such fluids has important impacts on heat transportation constant. Uncertainty nano liquids has advance heat conductive property related to simple base fluid and more have no insufficiency like density drops domination and destruction by nano size elements. Nano liquids had extraordinary useful in alarming of electric devices, transport, bio medication, atomic heat converter and several others. The leading continuation on nanofluid was pioneered by Choi [5] in 1995 which provides a direction to researchers to perform more work on this topic. Pal and Mandal [6] have discussed about mixed convective flow of nano-fluid radiation at stagnation point. Hayat et al. [7] have discussed about Erying nano-liquid on non-linear extending sheet of adjustable thickness. Makinde et al. [8] have discussed about the Brownian motion and Thermophoresis impact on mixed convection MHD flow of nano-liquids. Muhammad et al. [9] used convective approach to analyze the thermal properties of nanofluid in saturated porous space. Asma et al. [10] examined the effects of activation energy and chemical reaction applications in Darcy–Forchheimer flow of nanofluid induced by rotating disk. The numerical exploration for bioconvection assessment in Cross nanofluid confined by a moving wedge was intended by Muhammad et al. [11]. In another continuation, Muhammad et al. [12] focused on nonlinear thermally developed flow of 3-D Eyring-Powell nanofluid over a moving surface. Khan et al. [13] examined the effectiveness of bioconvection in nanoparticles over a flate surface confined by a moving free space. Zohra et al. [14] examined the heat transfer assessment in nanofluid under the effects of slip and gyrotactic microorganisms. Uddin et al. [15] implemented famous Chebyshev collocation scheme for a bioconvection flow problem under the dynamic consequences of magnetic induction and multiple slip constrains. Zohra [16] discussed the nanofluid fluid flow along with motile microorganisms over moving disk. Mahabaleshwar et al. [17] analyzed the nanofluid properties assumed over a stretched configuration with suction features. Ghasemian et al. [18] used Buongiorno nanofluid model to examine the heat transfer characteristics in 3-D rate type (Maxwell fluid) model. The work of Sreedevi [19] deals with interaction of gold and silver nanoparticles in Ethylene glycol base material to enhance the thermal performances. The resulted problem was tackled by using finite element technique. Some more recent work on thermal characteristics of nano-materials can be shown in refs. [20-23].

In various practical applications communication of forced convective thermal emission have many importance. Definitely, transmission of heat is more significant in increasing temperature radiation depending on the energy of the radiation particles which ionizing the fluid molecules and break down chemical bond. Several procedures in scheming regions occur at maximum temperature and information of heat energy transfer goes over to be commanding for the plan of the suitable equipment's. Rahman et al. [24] explained the results of transfer of heat in micro-polar liquid with a disposed porous sheet with different characteristics of fluid. Rahman et al. [25] discussed about the transfer of heat in a micropolar liquid with linear stretchable surface with a temperature dependent thickness and inconstant temperature of surface. Seddeek et al. [26] described the results of biochemical process and changeable thickness on mixed convective mass and heat transfer for flow through permeable sheet with radiation. In the field of engineering the transportation of thermal radiation have many importance in some applications such as solar influence accumulators, astral flows, huge open water tanks, heating and cooling chambers, and various other manufacturing and conservation developments. Incident radiations absorbed by nano-particles. Bakiers [27] discussed the effects of thermal radiation in mixed convection flow over a vertical plate. Damseh [28] observed the results of transverse magnetic field and transmission of heat radiation implement numerical study of magneto hydrodynamics mixed convection. Hossain and Takhar [29] examined the impacts of heat transfer radiation through forced and free convection. The phenomena of travelling heat waves in all direction are termed as thermal radiation. Moradi et al. [30] explained the streamlines are nearly corresponding to the vertical partitions on an inclined smooth surface and analysis of thermal emission, pressure and buoyant forces interaction.

The thermophoretic force is generated because of less vaporizer particle of in the existence of a temperature gradient. Thermophoresis is the motion of elements in the presence of this force. Thermophoresis is a tool of micro size element movement due to the temperature gradient and have many applications in vaporizer technology. Particularly this appliance is significant in deposition of particle against wafer in micro-electronics manufacturing, particle surfaces formed by condense vapor–gas mixture and many others in nuclear reactor safety. Thermophoretic laws are exploited to production classified catalogue germanium dioxide and silicon dioxide. In the field of transportations photosensitive fiber used. Chamkha et al. [31] measured the dual dimension natural convection flow on a smooth surface in the existence of thermophoresis and heat generation/absorption. Muhaimin et al. [32] explained the mass and transfer of heat of 2D mixed convective flow of viscous fluid. Moreover the measured the chemical reaction and thermophoresis also changeable stream situations. Noor et al. [33] calculated the MHD and thermophoresis flow of viscous liquid on tending sheet with heat generation/absorption and heat radiation. Anbuchezhian et al. [34] study to examine the thermophoresis properties and Brownian movement in the existence of boundary layer nanofluid.

For explaining the engineering and physical problems there are several investigative methods. The most useful solution technique for complicated modeled problems is successfully engaged by homotopic analysis method (HAM). The short coming of different solution techniques exploits the constraints which offer more complexity in the solutions. Among other investigative methods, homotopic scheme is best for any large consideration. HAM offers us to take early suppositions and supporting constraints to hold and modify the converging section that is the essential for some other measures [35-41].

Above all, the main consideration of current contribution is to examine the influences of heat and mass transfer effects in flow of magneto-Walter's B nanofluid under the effects of buoyant forces, thermophoretic applications, Joule heating and nonlinear thermal radiation. The thermal radiation consequences are considered nonlinear which make the problem quite versatile. The non-Newtonian Walter's B fluid exhibits the viscoelastic effects.

2. Mathematical presentation of problem

We study the steady 2D flow of Magneto-Walter B nanofluid over stretching sheet where pressure and buoyant forces act together. The particle deposition with thermophoresis and chemical reaction has been incorporated. The magnetic field effects are considered along vertical direction where induced magnetic force effects are neglected under the lower magnetic Reynolds number assumptions. The energy equation is modified in view of thermal radiation and Joule heating consequences. Moreover, the thermophoretic effects and chemical reaction features are taken into account the in concentration equation (See Fig. 1).

The governing equations of continuity, momentum, energy and concentration for the present flow of analysis given as [41]

$$u_x + v_y = 0, \tag{1}$$

$$uu_x + vu_y = \frac{\mu_\circ}{\rho_f}(u_{yy}) - \frac{k_\circ}{\rho_f}\begin{pmatrix} uu_{xyy} + vu_{yyy} \\ -u_y u_{xy} + u_x u_{yy} \end{pmatrix} - \frac{\sigma}{\rho_f}B_0^2 u + \frac{1}{\rho_f}[g(\beta_T(T-T_\infty) + \beta_C(C-C_\infty))], \tag{2}$$

$$uT_x + vT_y = \alpha T_{yy} + \frac{16\sigma^*}{3k^*(\rho C_p)_f}\left(T^3 T_y\right)_y + \frac{\sigma B_0^2 u^2}{(\rho C_p)_f} + \tau\left(D_B C_y T_y + \frac{D_T}{T_\infty}\left(T_y\right)^2\right) + \frac{Q_0}{(\rho C_p)_f}(T - T_\infty), \tag{3}$$

$$uC_x + vC_y = D_B C_{yy} + \frac{D_T}{T_\infty}T_{yy} - (V_T(C - C_\infty))_y - k(C - C_\infty). \tag{4}$$

where (u, v) velocity components along x and y axes, $k_\circ$ material parameter, ρ_f base fluid density, g acceleration due to gravity, σ electric conductivity, T is temperature, B magnetic field strength, σ^* Stefan Boltzmann constant, D_T thermophoretic diffusion coefficient, D_B Brownian diffusion coefficient, Q_0 is heat source coefficient, V_T thermophoretic velocity $(\rho C_p)_f$ heat capacity of fluid, C nanofluid concentration, and k^* notify absorption constant.

For the present flow analysis, the related boundary conditions are given as [41]:

$$\left.\begin{array}{c} u = u_w(x) = cx,\ v = 0,\ -kT_y = h_1\left(T_f - T\right), \\ -D_B C_y = h_2\left(C_f - C\right) \quad at\ y = 0, \\ u \to 0,\ \ T \to T_\infty,\ \ C \to C_\infty\ \ as\ \ y \to \infty. \end{array}\right\} \tag{5}$$

Taking the similarity transformation

$$\left.\begin{array}{lll} \xi = y\sqrt{\frac{c}{v}}, & u = cxH_\xi, & v = -\sqrt{cv}H, \\ \theta(\xi) = \frac{T-T_\infty}{T_f - T_\infty}, & \phi(\xi) = \frac{C-C_\infty}{C_f - C_\infty}, & V_T = -\frac{k^* v}{T_r}. \end{array}\right\} \tag{6}$$

The transformed flow problem is given as follows [41]

$$H_{\xi\xi\xi} - H_\xi^2 + HH_{\xi\xi} - \beta\left(2H_\xi H_{\xi\xi\xi} - H_{\xi\xi}^2 - HH_{\xi\xi\xi\xi}\right) - MH_\xi + \lambda(\theta + N\phi) = 0, \tag{7}$$

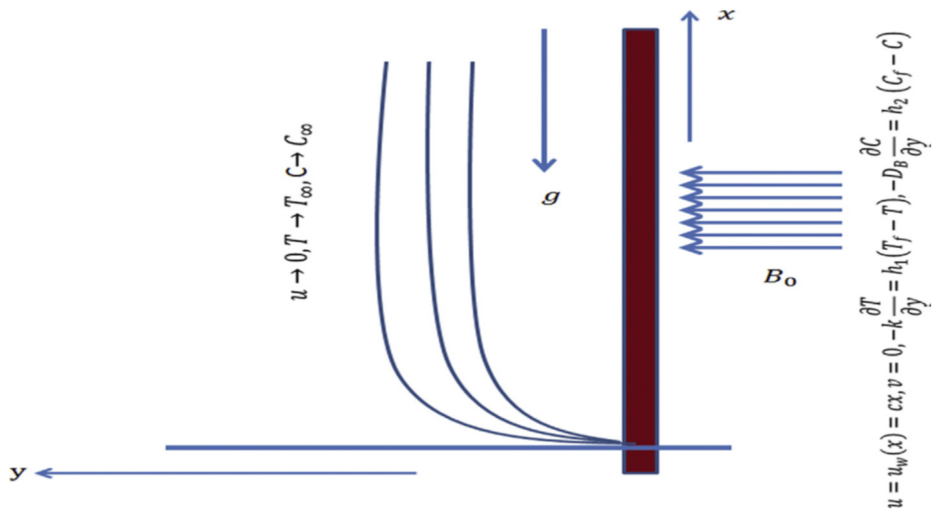

Fig. 1 Flow configuration for current model.

$$\left(\left(1+\frac{4}{3}R\left(1+(\theta_f-1)\theta\right)^3\right)\theta_\xi\right)_\xi + Pr\left(H\theta_\xi + M^2EcH_\xi^2 + N_b\theta_\xi\phi_\xi + N_t\theta_\xi^2 + \delta\theta\right) = 0 \tag{8}$$

$$\phi_{\xi\xi} + ScH\phi_\xi + \frac{Nt}{Nb}\theta_{\xi\xi} + J\mathrm{Pr}Le\theta_\xi\phi - \eta Sc\phi = 0 \tag{9}$$

$$\left.\begin{array}{l} H(0)=0,\ H_\xi(0)=1,\ \theta_\xi=-\gamma_1(1-\theta(0)),\ \phi_\xi=-\gamma_2(1-\phi(0)), \\ H\to 0,\ \theta\to 0,\ \phi\to 0,\ as\ \xi\to\infty. \end{array}\right\} \tag{10}$$

The non-dimensional parameters are defined as

$$\beta = \frac{k_0 c}{\mu_0}, \quad M^2 = \frac{\sigma B_0^2}{\rho_f c}, \quad \lambda = \frac{Gr_x^*}{Re_x^2},$$
$$Le = \frac{\alpha}{D_B}, \quad \eta = \frac{k}{c},$$

$$J = \frac{k^*(T_f - T_\infty)}{T_\infty}, \quad Re_x = \frac{xu_w(x)}{v}, \quad \mathrm{Pr} = \frac{v}{\alpha},$$
$$R = \frac{4\sigma^* T_\infty^3}{k^* k}, \quad \theta_f = \frac{T_f}{T_\infty},$$

$$N_b = \frac{\tau D_B(C_f - C_\infty)}{v}, \quad N_t = \frac{\tau D_T(T_f - T_\infty)}{T_\infty v},$$
$$Ec = \frac{u_w^2}{(C_p)_f(T_f - T_\infty)}, \quad Sc = \frac{v}{D_B},$$

$$\gamma_1 = \frac{h_1}{k}\sqrt{\frac{v}{\alpha}}, \quad \gamma_2 = \frac{h_2}{D_B}\sqrt{\frac{v}{\alpha}}, \quad \tau = \frac{(\rho C_p)_p}{(\rho C_p)_f},$$
$$\delta = \frac{Q_o}{c(\rho C_p)_f}.$$

In this expression β is the material parameter, M is the Hartman number, λ is thermal buoyancy parameter, η is the chemical heat generation parameter, Le is the Lewis number, J is the thermophoretic parameter, Pr is the Prandtl number, R is the thermal radiation parameter, N_b is the Brownian motion parameter, N_t is the thermophoresis parameter, Ec is the Eckert numberγ_1 is the thermal Biot number, δ is the heat generation parameter and Sc is the Schmidt number. It is remarked that $(\beta > 0)$ reflects the elastic-viscous material while $(\beta < 0)$ is associated with second grade fluid.

3. Homotopy analysis scheme

The formulated set formulated flow equations (7)-(9) with boundary conditions (10) are analytically proceeded by using homotopy analysis method. Due to familiar approach of this analytical scheme, the detail of solution has not presented here. Therefore, in section, we discuss the convergence analysis for employed scheme.

4. Convergence analysis

In homotopy analysis method, the auxiliary parameters $\hbar_H, \hbar_\theta$ and $\hbar_\phi$ are important to control and adjust the convergence of the resultant sequences solution. Therefore, we have drawn the so called $\hbar$-curves in Fig. 2(a)-(c) for three different orders of approximation for finding the acceptable ranges of $\hbar_H, \hbar_\theta$ and$\hbar_\phi$ which are $-1.2 \leqslant \hbar_H \leqslant 0.2$, $-3.5 \leqslant \hbar_\theta \leqslant 1.0$ and $-3.2 \leqslant \hbar_\phi \leqslant 1.5$. Table 1 describes the mathematical values of $H_{\xi\xi}(0)$, $\theta_\xi(0)$ and $\phi_\xi(0)$ for different orders of approximation. The calculation also indicates that the suitable values of $\hbar_H, \hbar_\theta$ and $\hbar_\phi$ are$\hbar_H = -0.5$,$\hbar_\theta = -1.0$ and$\hbar_\phi = -1.5$. Table 2 presents the solution verification by comparing present analysis with Ali et al. [42] and Akbar et al. [43] as a limiting case. It is noted that obtained numerical results show excellent agreement with these studies.

5. Discussion

In this segment our interest lies to express graphically the outcomes of velocity $H(\xi)$, temperature $\theta(\xi)$ and concentration profiles $\phi(\xi)$obtained by HAM for various involved parameters. For this task, Figs. 2–14 have been plotted by varying flow parameters. It is remarked that when each parameter get vary, the remaining flow parameters assign fixed numerical values. It is remarked that whole graphical analysis has been performed at 6th order of approximations.

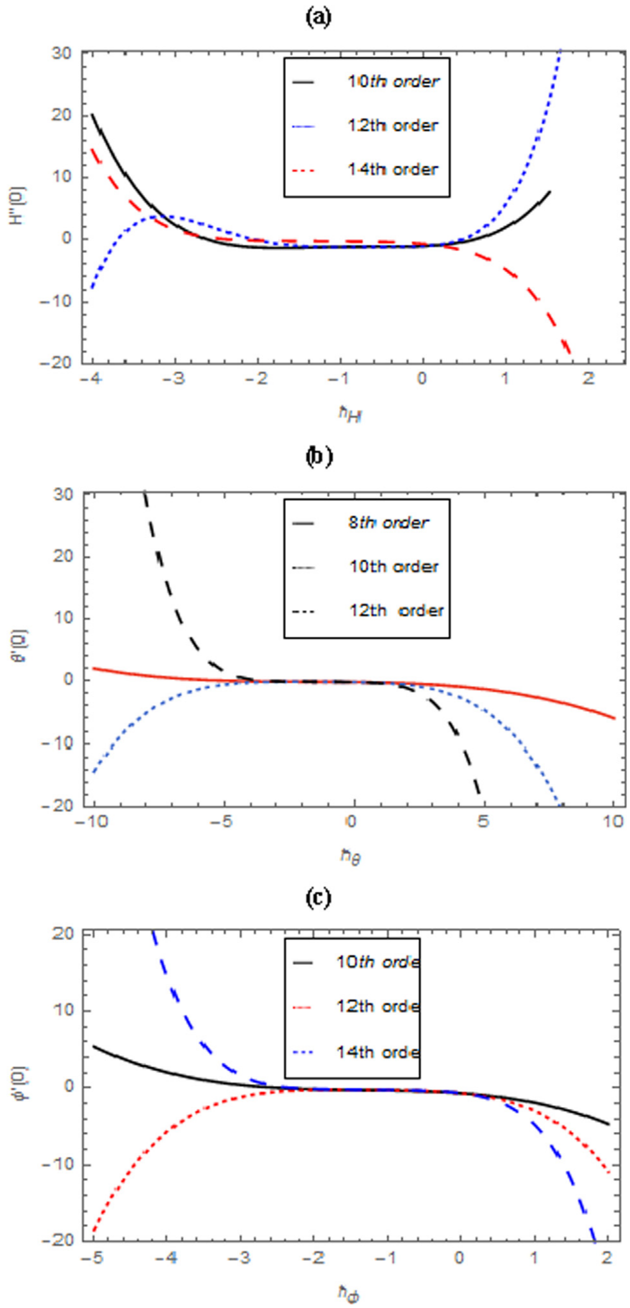

Fig. 2 h-curves for $H''(0), \theta'(0)$ and $\phi'(0)$.

Table 1 Convergence analysis for obtained solution.

Order of approximation	$H_{\xi\xi}(0)$	$\theta_\xi(0)$	$\phi_\xi(0)$
5^{th}	−1.02125	−0.127836	−0.131048
8^{th}	−1.031	−0.122905	−0.120215
10^{th}	−1.0348	−0.11867	−0.116056
12th	−1.0355	−0.114962	−0.112452

5.1. Velocity profile

Fig. 3 shows the influence of viscoelastic parameter β on fluid velocity. It shows that velocity of fluid decreases as we increase the value of β. Physically, the leading values of viscoelastic parameter accomplish dominant viscosity due to which velocity reduces. The significances of Hartman number M on fluid velocity is shown in Fig. 4. The higher values of Hartman number are associated with stronger Lorentz force which reduces the fluid particles velocity effectively.

Table 2 Comparison of solution with Ali et al. [42] and Akbar et al. [43] when $\beta = \lambda = N = 0$.

M	Ali et al. [42]	Akbar et al. [43]	Present results
0.0	1.0000	1.0000	1.0000
1.0	1.4142	1.41421	1.41423
5.0	2.4495	2.44948	2.44946

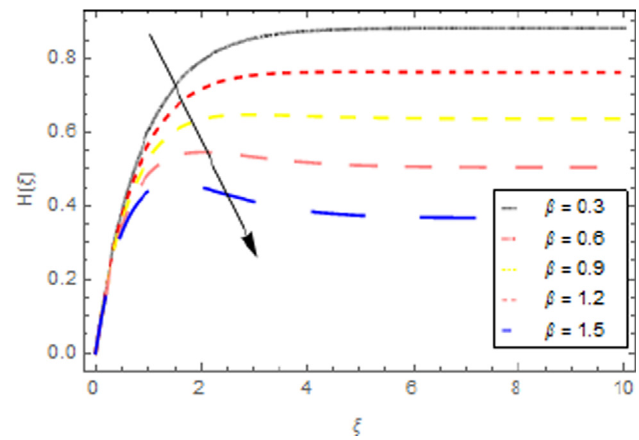

Fig. 3 Velocity profile for β when $J = 0.7$, $\delta = 0.2$, $R = 0.5$, $Pr = 0.7$ $Ec = 0.5$, $N_t = 0.1, R = 0.1$, $Le = 0.7$, $\eta = 0.5, M = 1.2$ and $Sc = 1.2$.

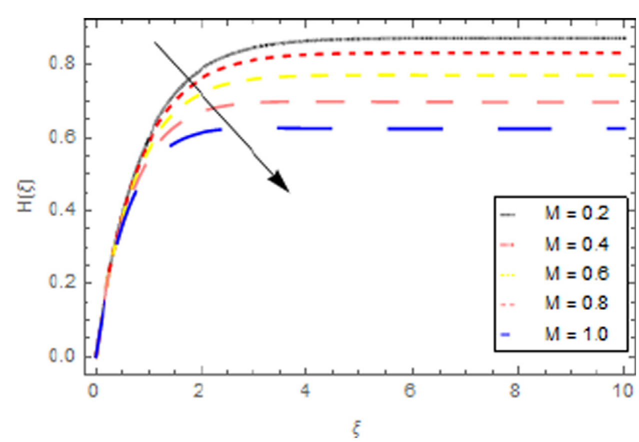

Fig. 4 Velocity profile for M when $J = 0.7$, $\delta = 0.2$, $R = 0.5$, $Pr = 0.7$ $Ec = 0.5$, $N_t = 0.1, R = 0.1, Le = 0.7$, $\eta = 0.5$, $\beta = 1.2$ and $Sc = 1.2$.

5.2. Temperature profile

The impact of Biot number γ_1 on $\theta$is given in Fig. 5. An arising magnitude of θ is noted due to increment in γ_1. The physical

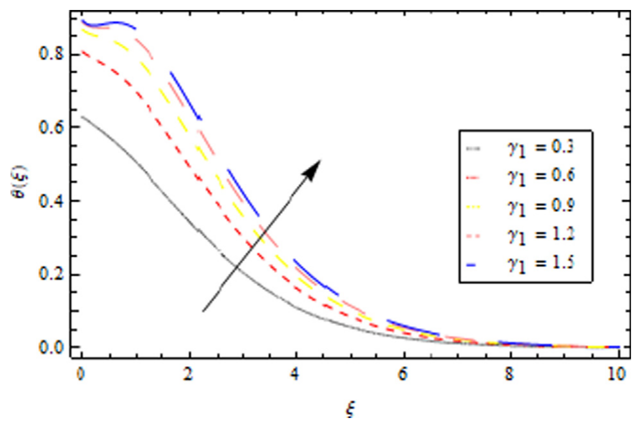

Fig. 5 Temperature profile for γ_1 when $J = 0.7$, $\delta = 0.2$, $R = 0.5$, $Pr = 0.7$ $Ec = 0.5$, $N_t = 0.1, R = 0.1$, $Le = 0.7$, $\eta = 0.5$, $\beta = 1.2$ and $Sc = 1.2$.

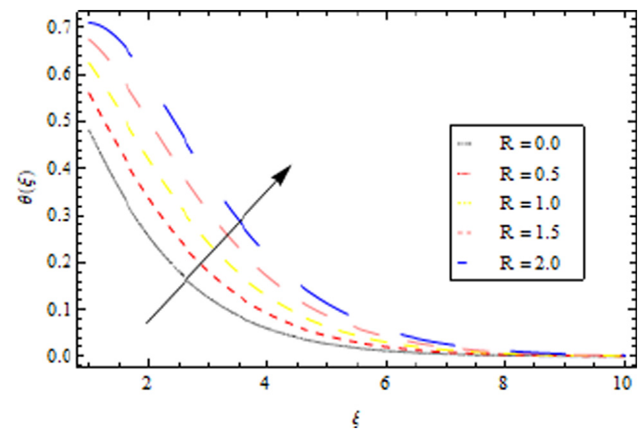

Fig. 8 Temperature profile for N_b when $J = 0.7$, $\gamma_1 = 0.5$, $\delta = 0.2$, $R = 0.5$, $Pr = 0.7$ $Ec = 0.5$, $N_t = 0.1, R = 0.1$, $Le = 0.7$, $\eta = 0.5$, $\beta = 1.2$ and $Sc = 1.2$.

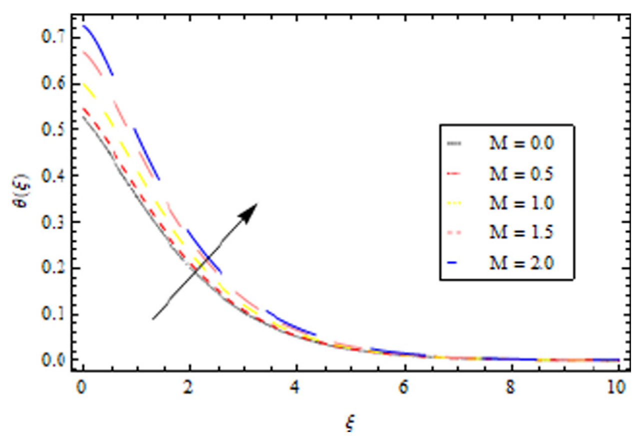

Fig. 6 Temperature profile for M when $J = 0.7, \gamma_1 = 0.5$, $\delta = 0.2$, $R = 0.5$, $Pr = 0.7$ $Ec = 0.5$, $N_t = 0.1, R = 0.1$, $Le = 0.7$, $\eta = 0.5, \beta = 1.2$ and $Sc = 1.2$.

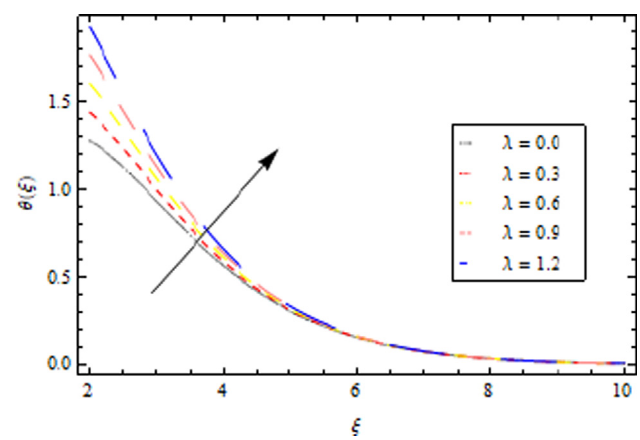

Fig. 9 Temperature profile for N_b when $J = 0.7$, $\gamma_1 = 0.5$, $\delta = 0.2$, $R = 0.5$, $Pr = 0.7$ $Ec = 0.5$, $N_t = 0.1, R = 0.1$, $Le = 0.7$, $\eta = 0.5$, $\beta = 1.2$ and $Sc = 1.2$.

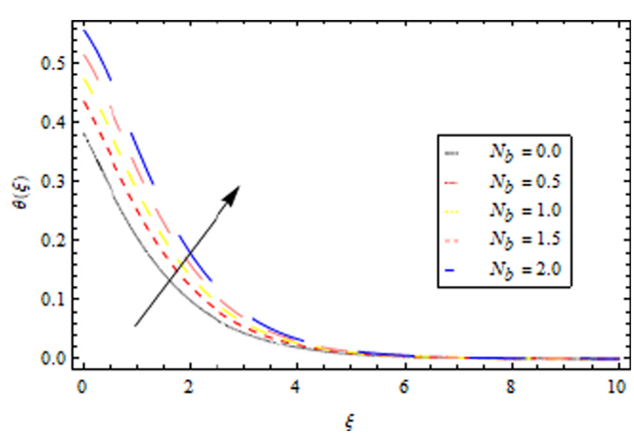

Fig. 7 Temperature profile for N_b when $J = 0.7, \gamma_1 = 0.5$, $\delta = 0.2$, $R = 0.5$, $Pr = 0.7$ $Ec = 0.5$, $N_t = 0.1, R = 0.1$, $Le = 0.7$, $\eta = 0.5$, $\beta = 1.2$ and $Sc = 1.2$.

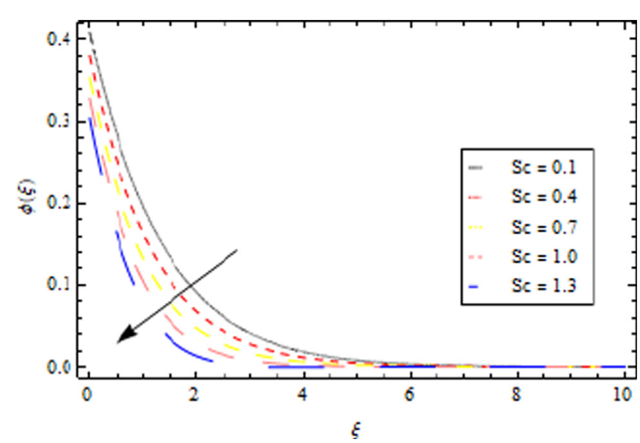

Fig. 10 Concentration profile for Sc when $J = 0.7$, $\gamma_1 = 0.5$, $\delta = 0.2$, $R = 0.5$, $Pr = 0.7$, $Ec = 0.5$, $N_t = 0.1, R = 0.1$, $Le = 0.7$, $\eta = 0.5$, $\beta = 1.2$ and $N_b = 1.2$.

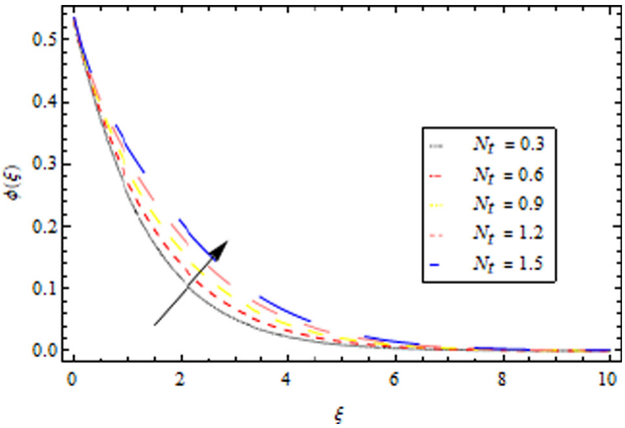

Fig. 11 Concentration profile for N_t when $J=0.7$, $\gamma_1=0.5$, $\delta=0.2$, $R=0.5$, $Pr=0.7$, $Ec=0.5$, $Le=0.7$, $\eta=0.5$, $\beta=1.2$ and $N_b=1.2$.

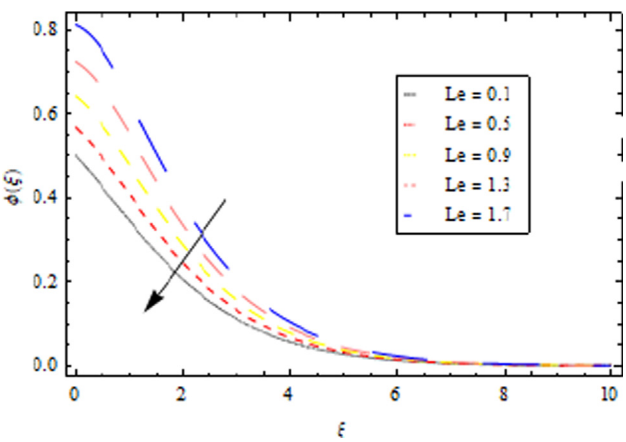

Fig. 12 Concentration profile for Le when $J=0.7, \gamma_1=0.5$, $\delta=0.2$, $R=0.5$, $Pr=0.7$ $Ec=0.5$, $N_t=0.1, R=0.1, Sc=0.7$, $\eta=0.5, \beta=1.2$ and $N_b=1.2$.

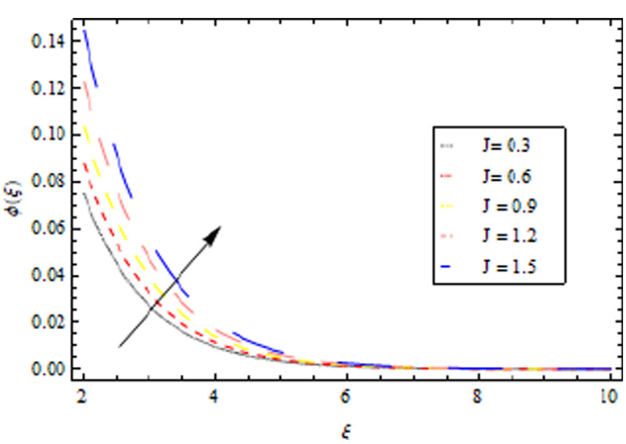

Fig. 13 Concentration profile for J when $Sc=0.7$, $\gamma_1=0.5$, $\delta=0.2$, $R=0.5$, $Pr=0.7$ $Ec=0.5$, $N_t=0.1, R=0.1$, $Le=0.7$, $\eta=0.5$, $\beta=1.2$ and $N_b=1.2$.

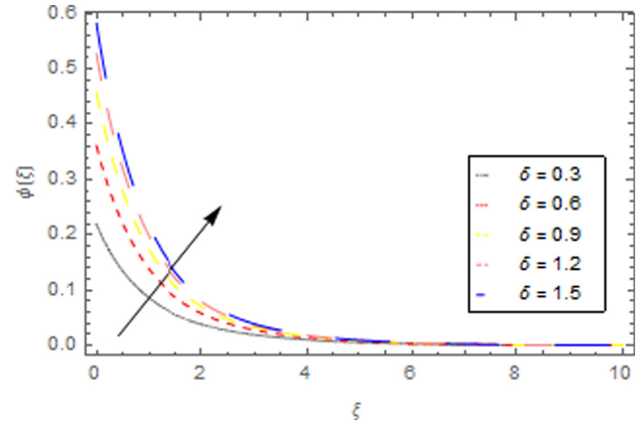

Fig. 14 Concentration profile for δ when $J=0.7$, $\gamma_1=0.5$, $Sc=0.2$, $R=0.5$, $Pr=0.7$, $Ec=0.5$, $N_t=0.1, R=0.1$, $Le=0.7$, $\eta=0.5$, $\beta=1.2$ and $N_b=1.2$.

justification behind such increasing temperature distribution is attributed as Biot number is related to the coefficient of heat transfer due to which temperature enhanced. The impact of M on θ is shown in Fig. 6. The temperature of fluid rises with M. The physical significances of such improved temperature is related to the Lorentz force effects. The interaction of Lorentz force improves the nanofluid temperature. The influence of N_b on $\theta$is shown in Fig. 7. It shows that the fluid temperature upsurge as we increase the value of N_b. The Brownian movement reveals with random movement of fluid particles within the heated system. When Brownian constant increases, it enhances the fluid particles movement due to which a maximum temperature is achieved. The stimulus of radiation constant R on θ is shown in Fig. 8. The temperature of fluid and thermal layer is maximum for growing value of R. The utilization of thermal radiation exhibit more thermal energy to the heated fluid particles which results an increment in θ. The impact of λ on θ is shown in Fig. 9. The temperature profile rises as we rise the value of λ.

5.3. Concentration profile

The outcomes of Schmidt number Sc on $\phi$are shown in Fig. 10. Enlarge change in Sc reports a decreases in the nano-particles concentration. The change in Schmidt number gets lower solutal diffusion which notify a reduced nanofluid concentration. The impact of N_t on $\phi$is shown in Fig. 11. The ϕenhances when we enhance the value of N_t. The manipulate of Le on ϕ is plotted in Fig. 12. The profile of concentration decreases when we upsurge the value of Le. The influence of J on ϕ is plotted in Fig. 13. The profile of concentration upsurge for leading values of J. The impact of heat generation parameter δ on $\phi$is shown in Fig. 14. The concentration profile shows increasing behavior with δ.

6. Conclusions

In this theoretical contribution, we have analyzed the enhancement of heat and mass transfer characteristics in flow of magnetized Walter's B nanofluid by using Buongiorno nanofluid model. The significant of Joule heating, chemical reaction and non-linear thermal radiation are also utilized to improve the thermal transport process. In contrast to traditional analysis, thermal and solutal convective conditions are employed to examine the thermal transport analysis. The outcomes have been summarized as follow

- A lower velocity assessment is noted with variation of viscoelastic parameter and Hratmann number.
- The consideration of thermal and solutal convective conditions is more useful to improve the nanofluid temperature.
- The Brownian motion, radiation parameter and thermophoretic constant improve the nano-material temperature.
- An improved concentration of nanofluid has been noticed with thermophoretic parameter and heat generation constant.
- The observation claimed from current thermal viscoelastic nanofluid model includes heat transportation, energy enhancement, thermal engineering, heating and cooling systems etc.
- The current results can be further extended for bioconvection flows, by using different non-Newtonian models and by utilizing distinct features like slip effects, entropy generation, activation energy, variable thermal conductivity, temperature dependent viscosity etc.

Acknowledgments

The research was supported by the National Natural Science Foundation of China (Grant Nos. 11971142, 11871202, 61673169, 11701176, 11626101, 11601485).

Appendix A. MATHEMATICA Code

```
GetRf[m_]: = Module[{temp},temp = fddd[m-1]-f1f1[m-1]
+ f0f2[m-1] + β (f2f2[m-1]-2f1f3[m-1] + f0f4[m-1])-
M*M*fd[m-1] + λ(g[m-1] + z*ϕ[m-1]);
Rf[m] = Expand[temp];];
GetRg[m_]: = Module[{temp},temp = (1 + 4/3*R)gdd[m-
1] + 4* R *ϵ *g1g1[m-1] + 8* R *ϵ2 *g0g1g1[m-1] + 4 *R
*ϵ3 *g0g0g1g1[m-1] + 4 *R *ϵ*g0g2[m-1] + 4 *R* ϵ2*
g0g0g2[m-1] + 4/3 *R* ϵ3*g0g0g0g2[m-1] + pr*(f0g1[m-
1] + M*M*Ec*f1f1[m-1] + Nb*g1ϕ1[m-1] + Nt*g1g1[m-
1] + α*g[m-1]);
Rg[m] = Expand[temp];];
GetRϕ[m_]: = Module[{temp},temp = ϕdd[m-1] + Sc*f0ϕ
1[m-1] + Nt/Nb*gdd[m-1] + J*pr*Le*g2ϕ0[m-1]-η*Sc*ϕ[
m-1];
Rϕ[m] = Expand[temp];];
GetInitialf: = Module[{},f[0] = 1-Exp[-y];];
GetInitialg: = Module[{},g[0] = γ/(1 + γ)*Exp[-y];];
GetInitialϕ: = Module[{},ϕ[0] = δ/(1 + δ)*Exp[-y];];
GetRHSf[m_]: = Module[{temp},GetRf[m];
RHSf[m] = Expand[TrigReduce[hbarf1*Rf[m]]];];
GetRHSg[m_]: = Module[{temp},GetRg[m];
RHSg[m] = Expand[TrigReduce[hbarg1*Rg[m]]];];
GetRHSϕ[m_]: = Module[{temp},GetRϕ[m];
RHSϕ[m] = Expand[TrigReduce[hbarϕ1*Rϕ[m]]];];
chi[m_]: = If[m < = 1,0,1];
GetAll[m_]: = Module[{},fd[m] = Expand[D[f[m],y]];
Lf[f_]: = Module[{},Expand[D[f,{y,3}]-D[f,y]]];
Lg[g_]: = Module[{},Expand[D[g,{y,2}]-g]];
Lϕ[ϕ_]: = Module[{},Expand[D[ϕ,{y,2}]-ϕ]];
Lfinv[f_]: = Module[{temp,EQ,u,w,solution,C1,C2},EQ =
Lf[u[y]]-f;
w = DSolve[EQ = = 0,u[y],y];
temp = w[[1,1,2]]/.C[_]- > 0;
C2 = D[temp,y]/.y- > 0;
C1 = –C2-temp/.y- > 0;
solution = temp + C1 + C2*Exp[-y];
Lginv[g_]: = Module[{temp,EQ,v,w,solution,C3,C4},EQ =
Lg[v[y]]-g;
w = DSolve[{EQ = = 0},v[y],y];
temp = w[[1,1,2]]/.C[_]- > 0;
(*temp1 = temp/.y∀0;*)
C3 = D[temp,y]/.y- > 0;
C4 = 1/(1 + γ) (C3-γ*temp/.y- > 0);
solution = temp + C4* Exp[-y];
Lϕinv[ϕ_]: = Module[{temp,EQ,v,w,solution,C5,C6},E
Q = Lϕ[v[y]]-ϕ;
w = DSolve[{EQ = = 0},v[y],y];
temp = w[[1,1,2]]/.C[_]- > 0;
(*temp1 = temp/.y∀0;*)
C5 = D[temp,y]/.y- > 0;
C6 = 1/(1 + δ) (C5-δ*temp/.y- > 0);
solution = temp + C6*Exp[-y];
Expand[solution]];
GetSpecialf[m_]: = Module[{temp},temp = Expand[RHSf
[m]];
Specialf = Lfinv[temp];];
GetSpecialg[m_]: = Module[{temp},temp = Expand[RHSg
[m]];
Specialg = Lginv[temp];];
GetSpecialϕ[m_]: = Module[{temp},temp = Expand
[RHSϕ[m]];
Specialϕ = Lϕinv[temp];];
Getf[m_]: = Module[{temp},temp[0] = Specialf + chi[m]*f
[m-1];
f[m] = Expand[temp[0]];];
Getg[m_]: = Module[{temp},temp[0] = Specialg + chi[m]
*g[m-1];
g[m] = Expand[temp[0]];];
Getϕ[m_]: = Module[{temp},temp[0] = Specialϕ + chi[m]
*ϕ[m-1];
ϕ[m] = Expand[temp[0]];];
ham[m0_,m1_]: = Module[{temp,m},For[m = Max[1,m0],
m < = m1,m = m + 1,Print[" m = ",m];
GetAll[m-1];
GetRHSf[m];
GetSpecialf[m];
Getf[m];
GetRHSg[m];
GetSpecialg[m];
Getg[m];
GetRHSϕ[m];
GetSpecialϕ[m];
Getϕ[m];
F[m] = F[m-1] + f[m];
G[m] = G[m-1] + g[m];
ϕϕ[m] = ϕϕ[m-1] + ϕ[m];
Print["F = ",F[m]];
Print["G = ",G[m]];
Print[" ϕ = ",ϕϕ[m]];
```

```
(*Fdd[m] = D[F[m],{y,2}]/.y∀0;
Gdd[m] = D[G[m],{y,1}]/.y∀0;
ϕϕd[m] = D[ϕϕ[m],{y,1}]/.y∀0;*)
(*Print["Fdd = ",Fdd[m]];*)
(*Print["Gdd = ",Gdd[m]];*)
(*Print["ϕϕd = ",ϕϕd[m]];*)
(*Plot[Fdd[m],{h,-2,0}]];*)
];
cpu[];
Print["Successful !"];];
GetInitialf;
GetInitialg;
GetInitialϕ;
F[0] = f[0];
G[0] = g[0];
ϕϕ[0] = ϕ[0];
hbarf1 = h1;
hbarg1 = h2;
hbarϕ1 = h3;
ham[1,19]
```

References

[1] K. Walters, Non-Newtonian effects in some elastic-viscous liquids whose behavior at small rates of shear is characterized by a general linear equation of state, Quart. J. Mech. Appl. Math. 15 (1) (1962) 63–76.

[2] M. Ijaz Khan, Faris Alzahrani, Aatef Hobiny, Heat transport and nonlinear mixed convective nanomaterial slip flow of Walter-B fluid containing gyrotactic microorganisms, Alex. Eng. J 59 (3) (2020) 1761–1769.

[3] Rahila Naz, Sana Tariq, Hamed Alsulami, Inquiry of entropy generation in stratified Walters' B nanofluid with swimming gyrotactic microorganisms, Alex. Eng. J. 59 (1) (2020) 247–261.

[4] SanaTariq RahilaNaz, Hamed Alsulami, Inquiry of entropy generation in stratified Walters' B nanofluid with swimming gyrotactic microorganisms, Alex. Eng. J. 59 (1) (2020) 247–261.

[5] S.U.S. Choi, Enhancing thermal conductivity of fluids with nanoparticles, ASME-Publications-Fed. 231 (1995) 99–106.

[6] D. Pal, G. Mandal, Mixed convection radiation on stagnation point flow of nanofluids over a stretching/shrinking sheet in a porous medium with heat generation and viscous dissipation, J. Pet. Sci. Eng. 126 (2015) 16e25.

[7] T. Hayat, I. Ullah, A. Alsaedi, M. Farooq, MHD flow of Powell-Eyring nanofluid over a non-linear stretching sheet with variable thickness, Results Phy. 7 (2017) 189e96.

[8] Makinde. O.D, Animasaun. I.L, Thermophoresis and Brownianmotion effects on MHD bio convection of nanofluid withnonlinear thermal radiation and quartic chemical reaction past an upper horizontal surface of a paraboloid of revolution, J Mol Liq; 221:733e43.

[9] Taseer Muhammad, Ahmed Alsaedi, Tasawar Hayat, Sabir Ali Shehzad, A revised model for Darcy-Forchheimer three-dimensional flow of nanofluid subject to convective boundary condition, Results Phys. 7 (2017) 2791–2797.

[10] Mir Asma, W.A.M. Othman, Taseer Muhammad, Numerical study for darcy–forchheimer flow of nanofluid due to a rotating disk with binary chemical reaction and arrhenius activation energy, Mathematics, 2019, 7(10), 921

[11] Taseer Muhammad, Sultan Z. Alamri, Hassan Waqas, Danial Habib, R. Ellahi, Bioconvection flow of magnetized Carreau nanofluid under the influence of slip over a wedge with motile microorganisms, J. Therm. Anal. Calorim (2020), https://doi.org/10.1007/s10973-020-09580-4.

[12] Taseer Muhammad, Hassan Waqas, Shan Ali Khan, R. Ellahi, Sadiq M. Sait, Significance of nonlinear thermal radiation in 3D Eyring-Powell nanofluid flow with Arrhenius activation energy, J. Therm. Anal. Calorim. (2020), https://doi.org/10.1007/s10973-020-09459-4.

[13] Waqar A. Khan, Md Jashim Uddin, A.I.Md. Ismail, Hydrodynamic and Thermal slip effect on double-diffusive free convective boundary layer flow of a nanofluid past a flat vertical plate in the moving free Stream, PLoS ONE 8 (3) (2013) e54024.

[14] Fatema T. Zohra, Mohammed J. Uddin, Ahamd I.M. Ismail, Magnetohydrodynamic bio-nanoconvective Naiver slip flow of micropolar fluid in a stretchable horizontal channel, Heat Trans. Asian Res. 48 (8) (2019) 3636–3656.

[15] , MJ Uddin, MN Kabir, O Anwar Bég, Y Alginahi, Chebyshev collocation computation of magneto-bioconvection nanofluid flow over a wedge with multiple slips and magnetic induction , Proceedings of the Institution of Mechanical Engineers, Part N: Journal of Nanomaterials, Nanoengineering and Nanosystems, Vol 232, Issue 4, 2018.

[16] Fatema Tuz Zohra, Mohammed Jashim Uddin, Md Faisal Basir, Magnetohydrodynamic bio-nano-convective slip flow with Stefan blowing effects over a rotating disc , Proceedings of the Institution of Mechanical Engineers, Part N: Journal of Nanomaterials, Nanoengineering and Nanosystems,Vol 234, Issue 3-4, 2020.

[17] U. S. Mahabaleshwar, P. N. Vinay Kumar and Mikhail Sheremet, Magnetohydrodynamics flow of a nanofluid driven by a stretching/shrinking sheet with suction, Springer Plus, volume 5, Article number: 1901 (2016).

[18] Amirhossein Ghasemian, Saeed Dinarvand, Armen Adamian, Mikhail A. Sheremet, Unsteady general three-dimensional stagnation point flow of a maxwell/buongiorno non-newtonian nanofluid, J. Nanofluids 8 (2019) 1544–1559.

[19] P. Sreedevi, P. Sudarsana Reddy, M.A. Sheremet, Impact of homogeneous–heterogeneous reactions on heat and mass transfer flow of Au–Eg and Ag–Eg Maxwell nanofluid past a horizontal stretched cylinder, J. Therm. Anal. Calorim. 141 (1) (2020) 533–546.

[20] B. Mallikarjuna, A.M. Rashad, Ahmed Kadhim Hussein, S. Hariprasad Raju, Transpiration and thermophoresis effects on non-darcy convective flow past a rotating cone with thermal radiation, Arab. J. Sci. Eng. 41 (11) (2016) 4691–4700.

[21] A.M. Rashad, B. Mallikarjuna, A.J. Chamkha, S. Hariprasad Raju, Thermophoresis effect on heat and mass transfer from a rotating cone in a porous medium with thermal radiation, Afrika Matematika 27 (2016) 1409–1424.

[22] Essam R. El-Zahar, Ahmed M. Rashad, and Laila F. Seddek, Impacts of Viscous Dissipation and Brownian Motion on Jeffrey Nanofluid Flow over an -Unsteady Stretching Surface with Thermophoresis, Symmetry, 12(9)(2020), 1450.

[23] S.R.R. Reddy, P. Bala Anki Reddy, A.M. Rashad, Activation energy impact on chemically reacting eyring-powell nanofluid flow over a stretching cylinder, Arab. J. Sci. Eng. 45 (7) (2020) 5227–5242.

[24] M.M. Rahman, A. Aziz, M.A. Al-Lawatia, Heat transfer in micro polar fluid alongan inclined permeable plate with variable fluid properties, Int. J. Therm. Sci. 49 (6) (2010) 993–1002.

[25] M.M. Rahman, M.A. Rahman, M.A. Samad, M.S. Alam, Heat transfer in a micropolar fluid along a non-linear stretching sheet with a temperature-dependent viscosity and variable surface temperature, Int. J. Thermophys. 30 (5) (2009) 1649–1670.

[26] M.A. Seddeek, A.A. Darwish, M.S. Abdelmeguid, Effects of chemical reactionand variable viscosity on hydromagnetic mixed convection heat and mass transfer for Hiemenz flow through porous media with radiation, Commun. Nonlinear Sci. Numer. Simul 12 (2) (2007) 195–213.

[27] A.Y. Bakier, Thermal radiation effect on mixed convection from vertical surface in saturated porous media, Int Commun Heat Mass Transf 28 (2001) 119–126.

[28] R.A. Damseh, Magnetohydrodynamics-mixed convection from radiate vertical isothermal surface embedded in a saturated porous media, J Appl Mech 73 (2006) 54–59.

[29] M.A. Hossain, H.S. Takhar, Radiation effect on mixed convection along a vertical plate with uniform surface temperature, Heat Mass Transf 31 (1996) 243–248.

[30] A. Moradi, H. Ahmadikia, T. Hayat, A. Alsaedi, On mixed convectionradiation interaction about an inclined plate through a porous medium, Int J Therm Sci 64 (2013) 129–136.

[31] A.J. Chamkha, A.F. Al-Muhaf, I. Pop, Effect of heat generation or absorption on thermophoretic free convection boundary layer from a vertical flat plate embedded in a porous medium, Int Commun Heat Mass Transfer. 33 (2006) 1096–1102.

[32] I. Muhaimin, R. Kandasamy, I. Hashim, Thermophoresis and chemical reaction effects on non-Darcy MHD mixed convective heat and mass transfer past a porous wedge in the presence of variable stream condition, Chem Eng Res Des. 87 (2009) 1527–1535.

[33] N.F.M. Noor, S. Abbasbandy, I. Hashim, Heat and mass transfer of thermophoretic MHD flow over an inclined radiate isothermal permeable surface in the presence of heat source/sink, Int J Heat Mass Transfer. 55 (2012) 2122–2128.

[34] N. Anbuchezhian, K. Srinivasan, K. Chandrasekaran, R. Kandasamy, Thermophoresis and Brownian motion effects on boundary layer flow of nanofluid in presence of thermal stratification due to solar energy, Appl Math Mech-Engl Ed. 33 (2012) 765–780.

[35] Liao, S.J., Advances in the Homotopy Analysis Method, World Scientific Publishing, 5 Toh Tuck Link, Singapore 2014.

[36] M. Turkyilmazoglu, Analytic approximate solutions of rotating disk boundary layer flow subject to a uniform suction or injection, Int. J. Mech. Sci.vol. 52 (2010) 1735–1744.

[37] M. Turkyilmazoglu, The analytical solution of mixed convection heat transfer and fluid flow of a MHD viscoelastic fluid over a permeable stretching surface, Int. J. Mech. Sci. 77 (2013) 263–268.

[38] Yu-Ming Chu, Samaira Aziz, Muhammad Ijaz Khan, Sami Ullah Khan, Mubbashar Nazeer, Iftikhar Ahmed, I. Tlili, Nonlinear radiative bioconvection flow of Maxwell nanofluid configured by bidirectional oscillatory moving surface with heat generation phenomenon, Physica Scripta, 95(10), 105007, (2020).

[39] Sami Ullah Khan, A Rauf, Sabir Ali Shehzad, Z. Abbas and T. Javed, Study of bioconvection flow in Oldroyd-B nanofluid with motile organisms and effective Prandtl approach, Physica A: Statistical Mechanics and its Applications, Volume 527, (2019), Article No. 121179.

[40] Muhammad Sadiq Hashmi, Nargis Khan, Sami Ullah Khan, M. Ijaz Khan, Thermophoretic particles deposition features in thermally developed flow of Maxwell fluid between two infinite stretched disks, Journal of Materials Research and Technology, Journal of Materials Research and Technology, Volume 9, Issue 6, November–December 2020, Pages 12889-12898.

[41] Tasawar Hayat, Arsalan Aziz, Taseer Muhammad , Ahmed Alsaedi , Model and Comparative Study for Flow of Viscoelastic Nanofluids with Cattaneo-Christov Double Diffusion, PLoS ONE 12(1): e0168824.

[42] F.M. Ali, R. Nazar, N.M. Arifin, I. Pop, MHD boundary layer flow and heat transfer over a stretching sheet with induced magnetic field, Heat Mass Transfer 47 (2) (2011) 155–162.

[43] N.S. Akbar, S. Nadeem, R.U. Haq, Z. Khan, Numerical solutions of Magnetohydrodynamic boundary layer flow of tangent hyperbolic fluid towards a stretching sheet, Indian J. Phys. 87 (11) (2013) 1121–1124.